PHYSICAL REVIEW B VOLUME 17, NUMBER 9 1 MAY 1978

# $^1$H and $^2$D NMR in stoichiometric PdH (PdD)

C. L. Wiley and F. Y. Fradin
*Argonne National Laboratory, Argonne, Illinois 60439*

(Received 28 November 1977)

The results of $^1$H and $^2$D nuclear spin-lattice relaxation-rate measurements in stoichiometric PdH and PdD, respectively, indicate an increasing spin density at the proton site, $[N(0)H_{\rm hfs}]_{\rm H}$, which correlates with the increase in $T_c$ with increasing hydrogen concentration. An isotope effect is also found $\{$i.e.,$[N(0)H_{\rm hfs}]_{\rm D}/[N(0)H_{\rm hfs}]_{\rm H} > 1\}$ for the stoichiometric compounds, which could result from the effect of the zero-point displacements smearing out the Fermi-level charge density at the hydrogenic sites.

## I. INTRODUCTION

Since the discovery of superconductivity in $PdH_x$ (a defect NaCl-type structure) by Skoskiewicz,[1] the changes in the electron and phonon structure of Pd upon hydriding, which yield an increase of $T_c$ from zero to ~10 K, have been a subject of a large volume of theoretical effort.[2-9] Most of the discussion has taken place with little or no experimental information on the electron and phonon structure of the $PdH_x$ system for values of $x$ near 1.0 where $T_c$ is nonzero. The experiments are difficult because of the extremely high pressure of $H_2$ that is required to establish equilibrium with the near stoichiometric composition at temperatures above 150 K. There is a lack of detailed understanding of the mechanism for the increase in $T_c$ with hydrogen concentration, the basis of the reverse isotope effect on $T_c$,[5] and the cause of the enhancement of $T_c$ when nontransitional impurities[10] are substituted in the Pd sublattice.

The present experimental investigation focuses on the use of $^1$H and $^2$D nuclear spin-lattice relaxation-rate measurements in stoichiometric PdH (PdD) to determine the normal-state electronic density of states at the Fermi level at the hydrogenic site. We have found an increase in the $s$ density of states at the Fermi level at the proton site $[N(0)H_{\rm hfs}]_{\rm H}$ as the concentration of hydrogen increases from 0.7 to 1.0. This increase correlates with the increase in $T_C$ and with the increase in $[N(0)H_{\rm hfs}]_{\rm H}$ predicted theoretically, but contrasts with the decrease in the total density of states at the Fermi level. We have also found a small but significant isotope effect on the measured spin-lattice relaxation rate (normalized by the square of the gyromagnetic ratio of the nucleus). That is, $[N(0)H_{\rm hfs}]_{\rm D}/[N(0)H_{\rm hfs}]_{\rm H} > 1$. We believe this indicates the importance of the zero-point vibrational motion on the time-average charge density at the Fermi level at the hydrogenic site.

## II. SAMPLE PREPARATION

Both the PdH and the PdD samples used in this experiment were prepared by an electrolytic charging process[11] in a three-electrode cell having an active volume of 500 ml and utilizing plane-parallel-plate geometry. A schematic diagram of this cell is shown in Fig. 1. The two outer electrodes (the anodes) consist of strips of 0.0015-in. Pt foil, $\frac{3}{4}$ in. wide by 10 in. long; the center electrode (the cathode) consists of a strip of 0.001-in. Pd foil, 1 cm wide by 8 in. long. Mechanical support of, and electrical contact to, the Pd strip is effected through 0.001-in. Pt tabs, 1 cm wide by 1–2 in. long, spot welded to each end of the Pd strip. All electrical connections within the cell are via Pt wires spot welded to the Pt foils. The Teflon electrode support maintains the anode-cathode spacing at $\frac{3}{4}$ in. and, by means of a threaded Teflon rod which connects the upper and lower segments of the electrode support, holds the two Pt anodes under tension. In order to maintain tension in the Pd electrode as its volume expands during hydrogenation, the lower end of the Pd strip is attached firmly (by means of a Teflon pin through the lower Pt tab) to the lower portion of the electrode support while the Pt tab at the upper end of the Pd electrode passes freely through a slot in the upper section of the electrode holder. Tension in the Pd electrode is maintained by means of a simple weight-and-pulley system attached to the Pt tab at the upper end of the Pd electrode.

The Pd foils were fabricated from Johnson Matthey 99.999% pure Pd (containing 1-ppm Fe) that was levitation melted and gas quenched in He to form an ingot which was subsequently rolled, in a manner to exclude iron contamination, into a foil 0.001 in. thick. After the foil was cut into strips 1 cm wide, the strips were strain-relief annealed in an evacuated (≈$10^{-5}$ Torr) furnace for 1 h at 750–850 °C.

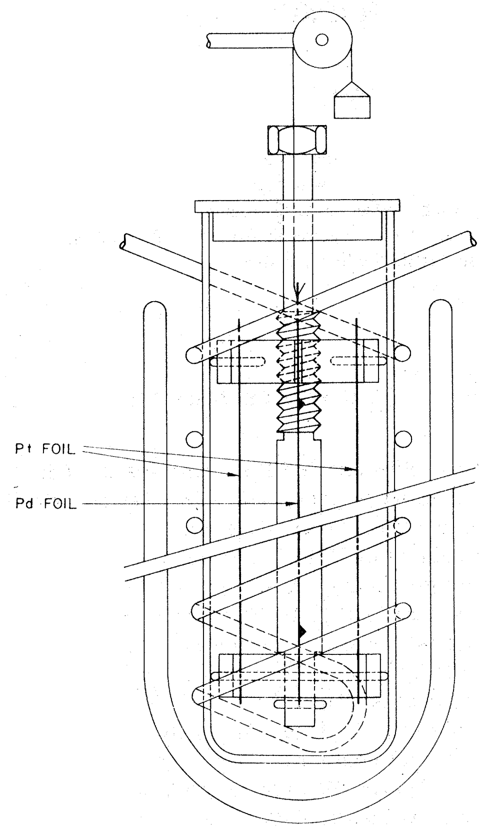

FIG. 1. Schematic diagram of the electrolytic-charging cell.

The essential difference between the preparation of a PdH sample and that of a PdD sample was in the electrolyte used during the charging process. To hydrogenate a Pd foil, the electrolyte consisted of 71 ml HCl (37% in $H_2O$) and 429 ml $CH_3OH$. To deuterate a Pd foil, the electrolyte consisted of 71 ml DCl (38% in $D_2O$) and 429 ml $CH_3OD$; the deuterated reagents used were at least 99 at. % isotopically pure deuterium. The electrolyte was discarded after one use.

During the charging process, the temperature of the electrolyte was held at a nominal temperature of −82 °C. Cooling of the electrolytic cell was effected by circulating the cold vapor from liquid nitrogen through a bifilar-wound coil of copper tubing that was wrapped around the exterior of the Pyrex charging cell. This assembly of cooling coil and charging cell was immersed in a low-temperature bath of acetone contained in an unsilvered dewar. The temperature of the coolant bath was monitored by a Cu-constantan thermocouple and was maintained constant within ±3 °C by a temperature controlling system that consisted of a Cu-constantan thermocouple connected to a Honeywell pyrovane temperature controller which actuated a solenoid valve in the supply line of the cold nitrogen vapor.

When the electrolyte had cooled to −82 °C, the Pd strip was anodized for 5–10 min at a current of 0.5 A. The electrolytic charging of the Pd foil was begun immediately after the anodizing process was terminated. The charging process was carried out in two steps. In the first step, to minimize the distortion of the Pd foil, charging currents during the initial stages of the charging process were limited to 0.5 A. Every 5–10 min during the early stages of the charging procedure, progress of the sample charging was monitored by a measurement of the Pd-foil resistance. These resistance measurements were made using a standard four-wire technique at an excitation current of 1 mA. The Pd-foil resistance as a function of charging time increases, reaches a maximum value (after approximately 20 min for PdH, 40 min for PdD), and finally decreases. The monitoring of the sample resistance was continued until the measurements showed no appreciable decrease in the Pd-foil resistance. In the second step, the charging current was increased to 1 A and the resistance monitoring was discontinued. After an additional time interval equal to approximately 70% of the length of time that sample charging proceeded at the initial current of 0.5 A, the current was increased from 1 to 1.5 A. The charging process was continued until a total charge of approximately 8 Ah had passed through the cell. The final one-half hour of sample charging was carried out at a current of approximately 2 A while the temperature of the electrolyte was being lowered to −95 °C. Although nearly stoichiometric samples could be obtained in the first charging step, we empirically found that the second step allowed us to reach hydrogen concentrations closer to unity and $T_c$'s higher than those previously reported.[5,12]

At the conclusion of the sample-charging process, the Teflon electrode support was quickly transferred to a liquid-nitrogen bath. The Pd foil was then cut free from the Pt tabs and transferred to a thermally insulated enameled tray containing liquid nitrogen. There the PdH (PdD) foil was scraped with forceps to remove any frozen electrolyte adhering to its surfaces. Finally, the sample foil was rolled (along with a $\frac{1}{2}$-in.-wide strip of 0.005-in. Teflon which served as an electrical insulator) onto a Teflon spool and secured in place with three bands of Belden No. 34 HNC Nyclad wire. This entire rolling procedure was performed with the PdH (PdD) sample under liquid nitrogen. The PdH (PdD) sample can be stored under liquid nitrogen for an indefinite period of time without degradation.

## III. EXPERIMENTAL MEASUREMENTS

The sample coil and the phase-sensitive detector of the nuclear-magnetic-resonance (NMR) spectrometer were used to measure the superconducting transition temperature $T_c$ at 18 and 8 MHz for the PdH and PdD samples, respectively. A calibrated Ge temperature sensor was used to determine the temperature of the sample. Figure 2 shows typical curves depicting the temperature dependence of the ac susceptibility in the vicinity of the superconducting transition for both the PdH and the PdD samples. As can be seen from this figure, the onset of the transition for both samples is well defined, but the low-temperature end of the transition is not well defined. Therefore, the width of the transition (measured between the 10% and the 90% amplitude points on the curve) is not a very reliable parameter to use for characterizing the superconducting transition of these samples. The $T_c$'s (corresponding to the onset of the transition) measured in this experiment are $T_c(\mathrm{PdH}) = 9.49 \pm 0.22$ K and $T_c(\mathrm{PdD}) = 11.59 \pm 0.14$ K. The corresponding widths $\Delta T_c$ of the transition are $\Delta T_c(\mathrm{PdH}) = 0.68 \pm 0.13$ K and $\Delta T_c(\mathrm{PdD}) = 0.42 \pm 0.08$ K. During each $T_c$ measurement, the temperature-dependence curve was traced twice—once while the sample temperature was being swept downward, and once while being swept upward. The hysteresis errors were less than ±0.25 K and ±0.05 K for the PdH and PdD samples, respectively.

Previous experience with the electrolytic charging procedure and measurement of the hydrogen concentration by gas evolution in a fixed-volume system indicates that the foils used in the NMR experiments have hydrogen-to-metal ratios of $0.995 \pm 0.005$. The values of $T_c$ are also consistent with values reported for nearly full stoichiometry.[5,12]

The NMR measurements were made at 18 and 8 MHz for the PdH and PdD samples, respectively, with a phase-coherent single-coil pulsed NMR spectrometer employing phase-sensitive detection. At these frequencies the external field is sufficiently large to quench the superconducting state. Radio-frequency magnetic fields of approximately 40 and 80 G were used for the NMR measurements on the PdH and PdD samples, respectively. A digital boxcar integrator or a Nicolet model 1074 digital signal averager with a Biomation model 802 fast digitizer was used to enhance the signal-to-noise ratio. The static magnetic field was supplied by a Varian electromagnet with Fieldial control. Measurements of the spin-lattice relaxation time $T_1$ were made at temperatures between 4.2 and 77 K by using a $\pi$-$\tau$-$\frac{1}{2}\pi$ pulse sequence and observing the recovery of the longitudinal magnetization $M(\tau)$. Single-exponential recovery was observed in all cases. Figure 3 shows typical recovery curves for both the PdH and the PdD samples.

A measure of the perfection of the NaCl-type structure of the PdD foil can be obtained from the free-induction decay (FID) of the $^2$D resonance. Figure 4 shows a typical FID curve which was fit to an $\exp(-t^2/2T_2^{*2})$ relation, yielding $T_2^* = 184$ $\mu$s. This value corresponds to a Gaussian line shape with second moment $\langle \Delta H^2 \rangle_{\mathrm{ex}} = 1.75$ G$^2$. The calculated dipolar second moment for the NaCl-type lattice is $\langle \Delta H^2 \rangle_{\mathrm{dip}} = 0.62$ G$^2$. Since $^2$D has a spin $I$

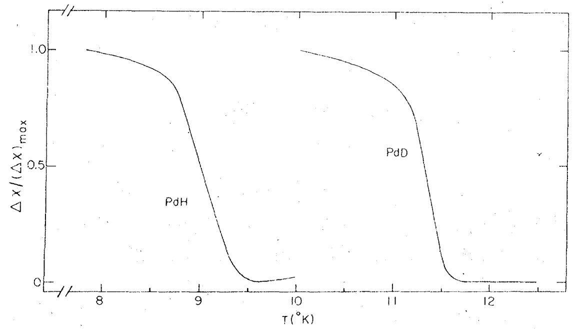

FIG. 2. Amplitude-normalized temperature dependence of the ac susceptibility in the vicinity of the superconducting transition for PdH at 18 MHz and for PdD at 8 MHz.

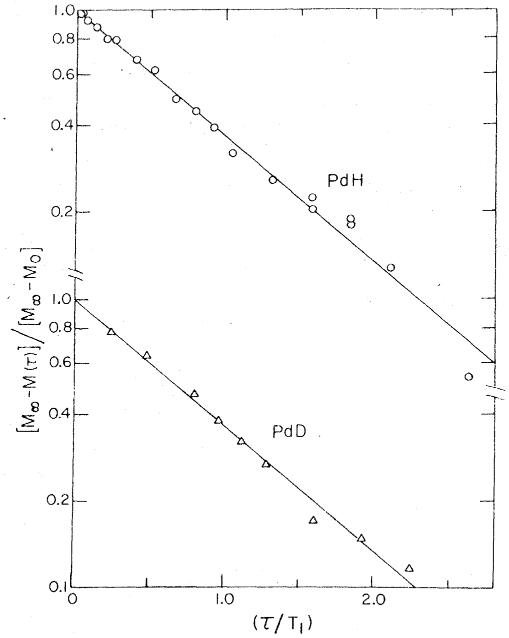

FIG. 3. Time-scale-normalized recovery curves of the longitudinal magnetization from its initial value $M_0$ to its equilibrium value $M_\infty$ at 4.2 K for PdH at 18 MHz and 4.2 kG [$T_1 = 4.99 \pm 0.18$ s] and for PdD at 8 MHz and 12.2 kG [$T_1 = 260 \pm 15$ s].

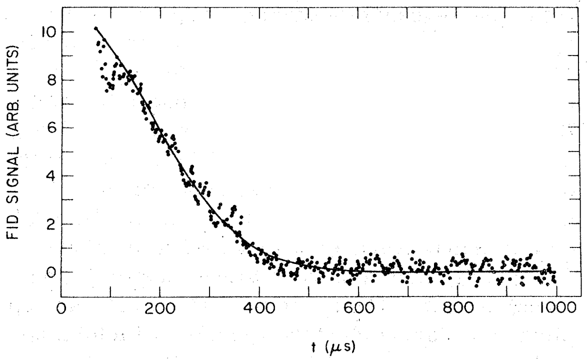

FIG. 4. Free-induction decay of $^2$D in PdD at 8 MHz, 12.2 kG, and 77 K. The solid curve is the function $\exp(-t^2/2T_2^{*2})$ with $T_2^* = 184$ μs. The signal-to-noise ratio has been enhanced by a factor of 8 due to signal averaging.

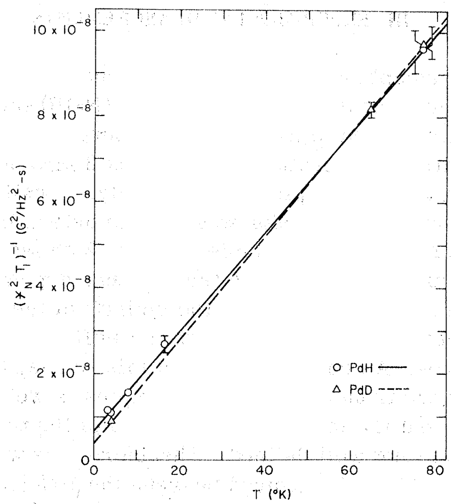

FIG. 5. $(\gamma_N^2 T_1)^{-1}$ vs $T$ for PdH at 18 MHz and 4.2 kG and for PdD at 8 MHz and 12.2 kG.

$= 1$ and a nuclear electric quadrupole moment $Q = 2.8 \times 10^{-3}$, there is rather good sensitivity for any defect that destroys the octahedral symmetry. If we associate the difference $\langle \Delta H^2 \rangle_{\mathrm{ex}} - \langle \Delta H^2 \rangle_{\mathrm{dip}}$ with the mean-squared quadrupolar splitting of the $^2$D line

$$\langle \Delta H^2 \rangle_Q = \tfrac{9}{400} (e^2 Q \bar{q}/\gamma h)^2 [(2I+3)/I^2(2I-1)],$$

we find a root-mean-square value of the electric field gradient of $\bar{q} = 2.1 \times 10^{22}$ cm$^{-3}$. Although a point-charge calculation usually underestimates the magnitude of $q$ in a metal, we present such a calculation for defective PdD to obtain an estimate of the upper limit for the defect concentration. A point-charge calculation of $q$ for 1 vacant deuterium site ($Z$ assumed equal to 1) in the 12 second-nearest-neighbor sites (at a distance $r = 2.89$ Å) yields $q_{\mathrm{pc}}^{\mathrm{vac}} = 8 \times 10^{22}$ cm$^{-3}$. This indicates that if the entire value of $\bar{q}$ was due to deuterium vacancies, we would have of order 2% vacant deuterium sites. This value is too large to be consistent with gas-evolution and $T_c$ measurements. However, a point-charge calculation of $q$ for a deuterium at one of the eight nearest-neighbor tetrahedral interstitial sites ($r = 1.77$ Å) yields $q_{\mathrm{pc}}^{\mathrm{int}} = 36 \times 10^{22}$ cm$^{-3}$, which implies 0.7% occupancy of the tetrahedral positions. This site occupancy is within the sensitivity of the refinement of elastic-neutron-scattering results.

TABLE I. Spin-lattice relaxation times for PdH at 18 MHz and 4.2 kG and for PdD at 8 MHz and 12.2 kG.

| Data for PdH | |
|---|---|
| $T$ (°K) | $T_1$ (s) |
| 3.28 | 4.76 ± 0.20 |
| 4.2 | 4.99 ± 0.18 |
| 8.09 | 3.51 ± 0.21 |
| 16.5 | 2.06 ± 0.15 |
| 77.0 | 0.576 ± 0.034 |
| **Data for PdD** | |
| $T$ (°K) | $T_1$ (s) |
| 4.2 | 262.0 ± 12.0 |
| 64.77 | 28.64 ± 0.63 |
| 77.0 | 24.14 ± 0.83 |

## IV. DISCUSSION OF RESULTS

In Table I we list the values of $T_1$ as a function of temperature for PdH and PdD. In Fig. 5, the temperature dependencies of $1/T_1$, normalized by the square of $\gamma$ (the nuclear gyromagnetic ratio divided by $2\pi$), for PdH and PdD are displayed. We note the close similarity of the results for the $^1$H and $^2$D relaxation rates. Least-squares fitting of the data in Fig. 5 to a constant plus a term linear in temperature yields

$$1/(T_1\gamma^2)_{\mathrm{H}} = [0.70(5) + 0.1154(14)T] \times 10^{-8}\ \mathrm{G^2/Hz^2\,s}, \tag{1}$$

$$1/(T_1\gamma^2)_{\mathrm{D}} = [0.38(3) + 0.1207(5)T] \times 10^{-8}\ \mathrm{G^2/Hz^2\,s}. \tag{2}$$

Here we have used the values $\gamma_{\mathrm{H}}^2 = 0.18128 \times 10^8$ (Hz/G)$^2$ and $\gamma_{\mathrm{D}}^2 = 0.42719 \times 10^6$ (Hz/G)$^2$. We see that in addition to a Korringa term ($1/T_1 \sim T$) in the relaxation rate there is a constant term. The size of the constant term is consistent with a paramagnetic-impurity contribution to the H (D) relaxation rate. If we assume that the fast nuclear-spin-diffusion regime is applicable and that relaxation proceeds due to transverse fluctuations of the paramagnetic impurity coupled via the nuclear dipole-electronic dipole interaction, then the values of the constant terms in Eqs. (1) and (2) are consistent with a concentration of order 1 ppm of paramagnetic impurity.[13] The impurity concentration appears to be about twice as large in PdH as in PdD, if everything else is assumed to be equal. The deviations from $T_1T$ = constant is a cause for concern in our analysis of the Korringa relaxation. However, we have not been able to prepare samples of higher purity. The linearity of the $T_1^{-1}$ data for PdH in Fig. 5 and the relative constancy of the intercept for PdH and PdD gives us confidence that the slope of the data in Fig. 5 yields the Korringa relaxation rate.

Korringa relaxation, which proceeds via the Fermi-contact hyperfine interaction of the Fermi-energy electrons at the H (D) nucleus, is given by

$$1/(T_1\gamma^{-2})_{\mathrm{H,D}} = 16\pi^3\hbar k_B T[N(0)H_{\mathrm{hfs}}]^2_{\mathrm{H,D}}, \tag{3}$$

where $N(0)$ is the density of states at the Fermi energy for one direction of spin and $H_{\mathrm{hfs}}$ is the one-spin Fermi-contact hyperfine field which is proportional to the square of the wave function at the H (D) nucleus averaged over the Fermi surface. The factorization of the hyperfine field in Eq. (3) is rigorous only for a spherical Fermi surface, where the square of the wave function is independent of the position on the Fermi surface. We have ignored exchange-enhancement effects in Eq. (3) since PdH (PdD) is diamagnetic.

Comparison of Eq. (3) with the term linear in $T$ in Eqs. (1) and (2) yields for the spin density at the H (D) site

$$[N(0)H_{\mathrm{hfs}}]_{\mathrm{H}} = 4.00(4)\times10^{15}\ \mathrm{G\,erg^{-1}} \tag{4}$$

and

$$[N(0)H_{\mathrm{hfs}}]_{\mathrm{D}} = 4.09(3)\times10^{15}\ \mathrm{G\,erg^{-1}}, \tag{5}$$

respectively. Whereas the errors indicated in Eqs. (1) and (2) represent one standard deviation, the errors given in Eqs. (4) and (5) are considerably larger and represent an estimate of the largest deviation that can reasonably be said to fit the data. The values in Eqs. (4) and (5) are also consistent with the fitted slope of only the $T > 4.2$-K data.

Recently Gupta and Freeman[14] have calculated the APW band structure for PdH. They have constructed densities of states and projections within the APW spheres at the Pd and H sites and have found a considerable piling up of charge at the hydrogen site. This charge serves to screen the potential of the proton. Gupta and Freeman have calculated the Fermi-surface average in the rigorous unfactorized form

$$[N(0)H_{\mathrm{hfs}}]_{\mathrm{theory}} = \frac{\Omega}{(2\pi)^3}\int_{\mathrm{FS}}\frac{dS_k}{|\nabla_k\epsilon_k|}|\psi_k^s(R_{\mathrm{H}})|^2 = 4.4\times10^{15}\ \mathrm{G\,erg^{-1}}, \tag{6}$$

where $\Omega$ is the atomic volume and $R_{\mathrm{H}}$ is the position of the hydrogen nucleus. This value is in fair agreement with the experimental value given in Eq. (4), being about 10% too large. If other spin-dependent contributions to $(T_1T)^{-1}$ were included, the gap between band theory and experiment would widen. Gupta and Freeman also calculate the ratio of the hyperfine field in PdH to that in atomic hydrogen $\xi = \langle|\psi(R_{\mathrm{H}})|^2\rangle_{\mathrm{FS}}/|\psi(R_{\mathrm{H}})|^2_{\mathrm{at}} = 0.267$ and the total density of states at the Fermi level in PdH, $N(0) = 3.4055\ \mathrm{Ry^{-1}\,spin^{-1}}$. Using $H^{\mathrm{at}}_{\mathrm{hfs}} = 167\times10^3$ G, we calculate the product $N(0)\ \xi H^{\mathrm{at}}_{\mathrm{hfs}} = 7.0\times10^{15}\ \mathrm{G\,erg^{-1}}$. We see that this value of the spin density, which assumes a spherical Fermi surface, is almost a factor of 2 larger than the experimental value. The experimental values of $N(0)H_{\mathrm{hfs}}$ thus indicate the importance of nonspherical Fermi-surface effects in PdH (PdD); as Gupta and Freeman indicate PdH is *not* a nearly free-electron material.

The 77-K lattice parameters of PdH (PdD) have been measured by Schirber and Morosin.[15] They find $a_0|_{\mathrm{PdH}} = 4.090$ Å and $a_0|_{\mathrm{PdD}} = 4.084$ Å, i.e., the atomic volume of the hydride is 0.4% larger than that of the deuteride. However, from Eqs. (4) and (5) the value of $N(0)H_{\mathrm{hfs}}$ for the deuteride is 2% larger than that for the hydride. Thus, we find a small but significant increase in the spin density at the deuterium site, an increase which is beyond the variation one would expect from the very small volume change. The significance of this isotope effect in the spin density at the H (D) site has been discussed by Jena *et al.*[16] It can be related to the larger zero-point displacements of the H relative to those of the D and the resultant smearing out of the self-consistent spin density (larger for H than for D) within about one Bohr radius of the equilibrium hydrogenic positions. The smearing effect would also bring the value of the band-theory spin density into better agreement with the experimental value. We have ignored the quadrupolar contribution[17] to $(T_1T)^{-1}$ for $^2$D. Estimates of this contribution, based on the quadrupolar contribution to the second moment, yield a value $<10^{-8}$ of the experimental rate. The lack of quadrupolar contribution to $T_1T$ is consistent with the fact that no quadrupolar effect is seen on $T_1T$ of $^{63,65}$Cu in metallic copper, where the quadrupolar effect, based on the nuclear gyromagnetic ratio and the nuclear quadrupolar moment, would be expected to be larger than in PdD.

In comparison to our results for the Korringa relaxation in stoichiometric PdH, Seymour *et al.*[18] find a value of $T_1T|_{\mathrm{PdH}_{0.70}} = 68 \pm 2$ s K and Arons *et al.*[19] find a value of $T_1T|_{\mathrm{PdH}_{0.73}} = 70$ s K. These results yield ~25% smaller values of $[N(0)H_{\mathrm{hfs}}]_{\mathrm{H}}$ than we have found for the stoichiometric PdH. Faulkner,[20] using a coherent-potential-approximation calculation for substoichiometric PdH, predicts an increase in the average density of states at the Fermi level at the hydrogen site on going from $\mathrm{PdH}_{0.7}$ to $\mathrm{PdH}_{\sim 1.0}$. Similarly, Klein *et al.*,[21] using a rigid-band argument based on their augmented-plane-wave calculation of the band structure of PdH, predict an increase in the *s* density of states at the Fermi level at the H (or D) site with increasing concentration of hydrogen. They show theoretically that an increase of $T_c$ is expected with increasing *s* density at the H site.

## V. CONCLUSION

$^1$H and $^2$D $T_1$ measurements in PdH and PdD indicate a strong dependence of the spin density at the hydrogenic site on hydrogen concentration. An isotope effect on the value of the spin density at the hydrogenic sites has also been found. There appears to be a correlation of the spin density at the hydrogenic site with the strength of the electron-phonon interactions.

## ACKNOWLEDGMENTS

The authors would like to thank A. J. Freeman and P. Jena for helpful discussions of their calculations, G. Cinader for experimental assistance, and D. G. Westlake for volumetric analysis of the hydrogen concentration. This work was supported by the U.S. Department of Energy.

---

[1] T. Skoskiewicz, Phys. Status Solidi A 11, K123 (1972).

[2] K. H. Bennemann and J. W. Garland, Z. Phys. 260, 367 (1973).

[3] S. Auluck, Nuovo Cimento Lett. 7, 545 (1973).

[4] P. Hertel, Z. Phys. 268, 111 (1974).

[5] R. J. Miller and C. B. Satterthwaite, Phys. Rev. Lett. 34, 144 (1975).

[6] J. S. Brown, Phys. Lett. A 51, 99 (1975).

[7] D. A. Papaconstantopoulos and B. M. Klein, Phys. Rev. Lett. 35, 110 (1975).

[8] B. N. Ganguly, Phys. Rev. B 14, 3848 (1976).

[9] D. S. McLachlan, T. B. Doyle, and J. P. Burger, J. Low Temp. Phys. 26, 589 (1977).

[10] B. Stritzker, Z. Phys. 268, 261 (1974).

[11] J. M. E. Harper, Phys. Lett. A 47, 69 (1974).

[12] J. E. Schirber and C. J. M. Northrup, Jr., Phys. Rev. B 10, 3818 (1974).

[13] See for example L. B. Welsh, C. L. Wiley, and F. Y. Fradin, Phys. Rev. B 11, 4156 (1975).

[14] M. Gupta and A. J. Freeman, Bull. Am. Phys. Soc. 22, 263 (1977).

[15] J. E. Schirber and B. Morosin, Phys. Rev. B 12, 117 (1975).

[16] P. Jena, C. L. Wiley, and F. Y. Fradin, Phys. Rev. Lett. 40, 578 (1978).

[17] Y. Obata, J. Phys. Soc. Jpn. 19, 2348 (1964).

[18] E. F. W. Seymour, R. M. Cotts, and W. D. Williams, Phys. Rev. Lett. 35, 165 (1975).

[19] R. R. Arons, H. G. Bohn, and H. Lütgemier, Solid State Commun. 14, 1203 (1974).

[20] J. S. Faulkner, Phys. Rev. B 13, 2391 (1976).

[21] B. M. Klein, E. N. Economou, and D. A. Papaconstantopoulos, Phys. Rev. Lett. 39, 574 (1977).